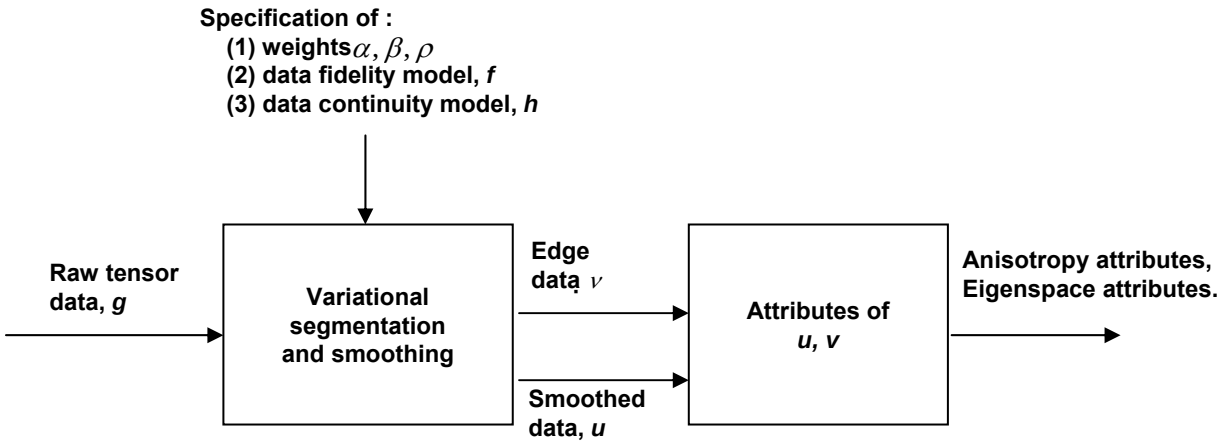

Figure 1: Block diagram of the variational segmentation processing framework. Variables refer to equation 1.

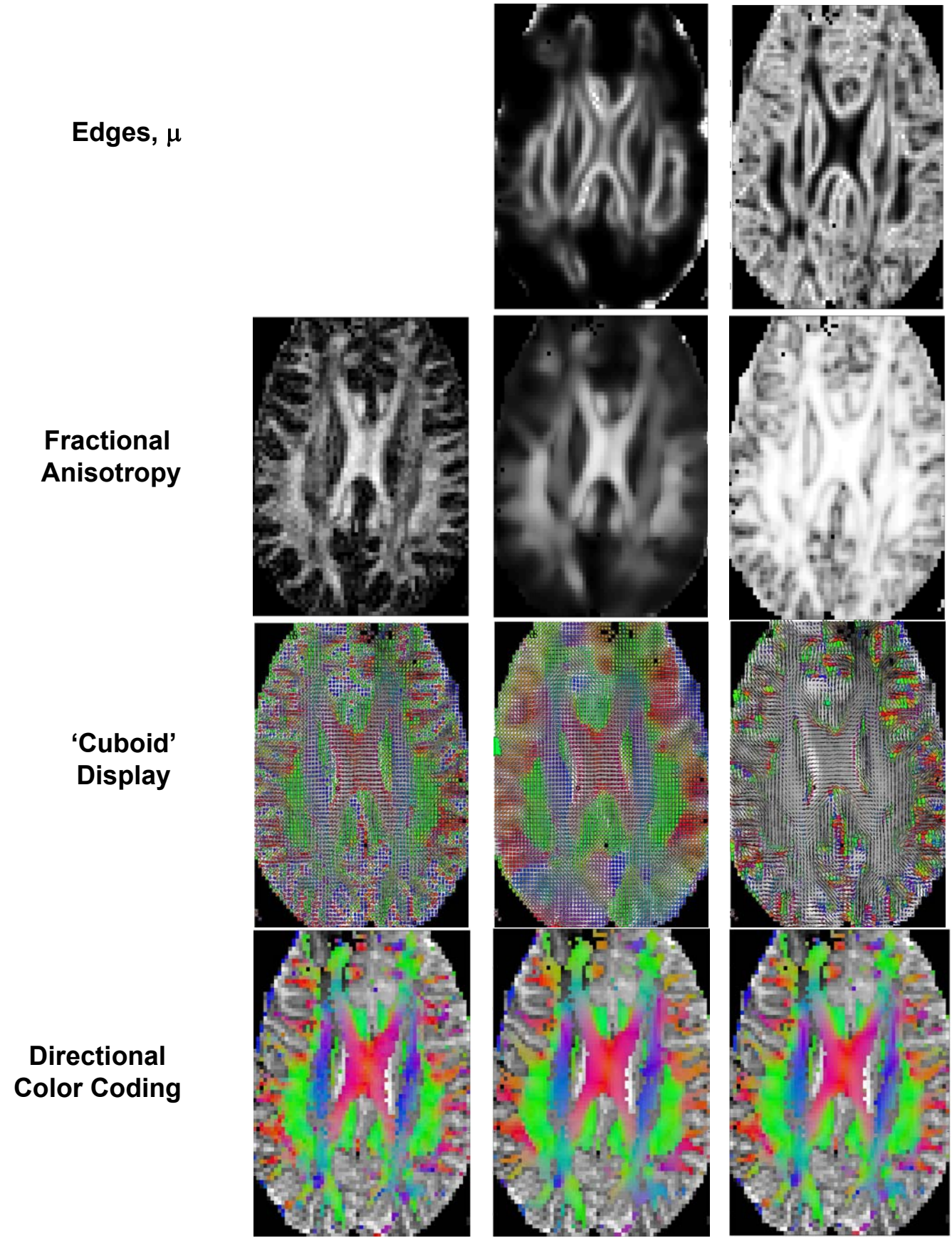
Edges, μ
Fractional Anisotropy
'Cuboid' Display
Directional Color Coding
Unsmoothed
Smoothed Normalized Tensor
Smoothed Directional Projection

Figure 2

Figure 2: Effect of two smoothing models (2nd and 3rd columns) on an axial brain slice. The fractional anisotropy and edge maps are displayed in the first two rows, and the 'cuboid' and color representations of the directional information contained in the resultant tensor fields are displayed in the last two rows. Maximum details emerge when smoothing is most selective, directional projection based (3rd column), within the edge field boundaries.

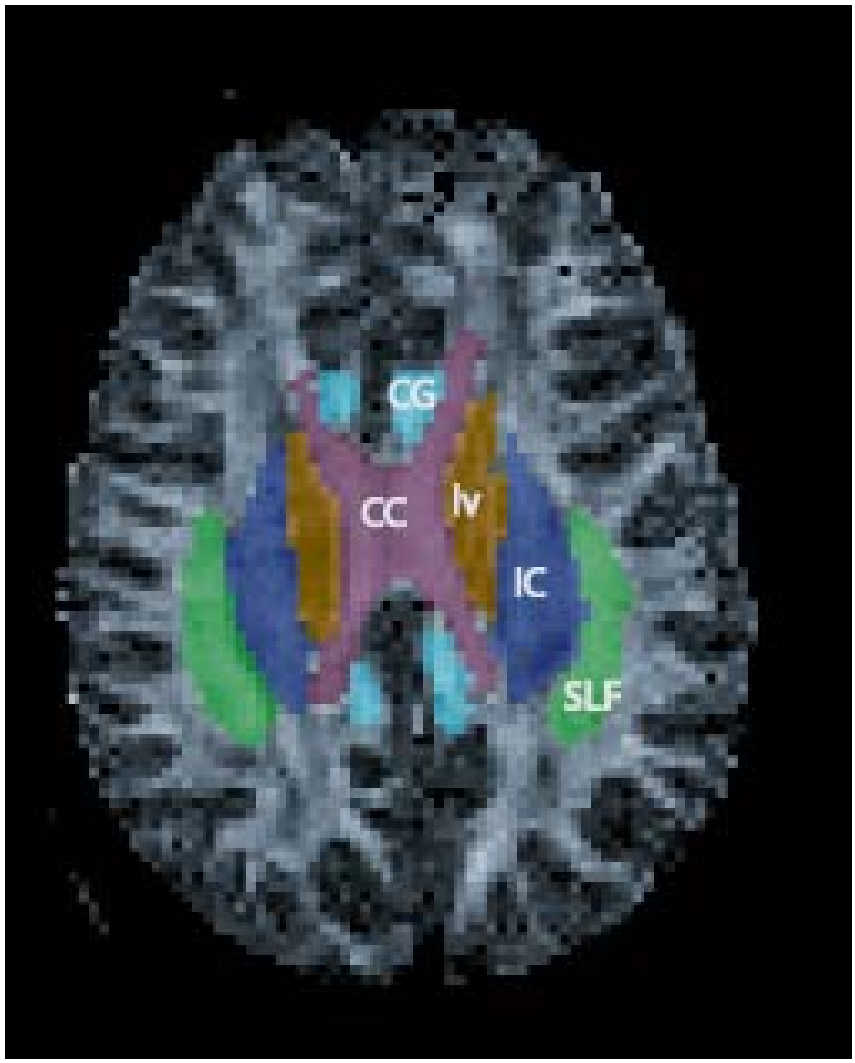

CC - corpus callosum
IC - internal capsule
SLF - superior longitudinal fasciculus
CG - cingulum bundle
lv - lateral ventricle

Figure 3: Manual delineation of five anatomically motivated regions for further analysis of impact of different modes of smoothing and segmentation on fractional anisotropy of smoothed tensor in the regions. Delineations were based upon tensor orientation and anisotropy, and are shown with respect to the fractional anisotropy map here.

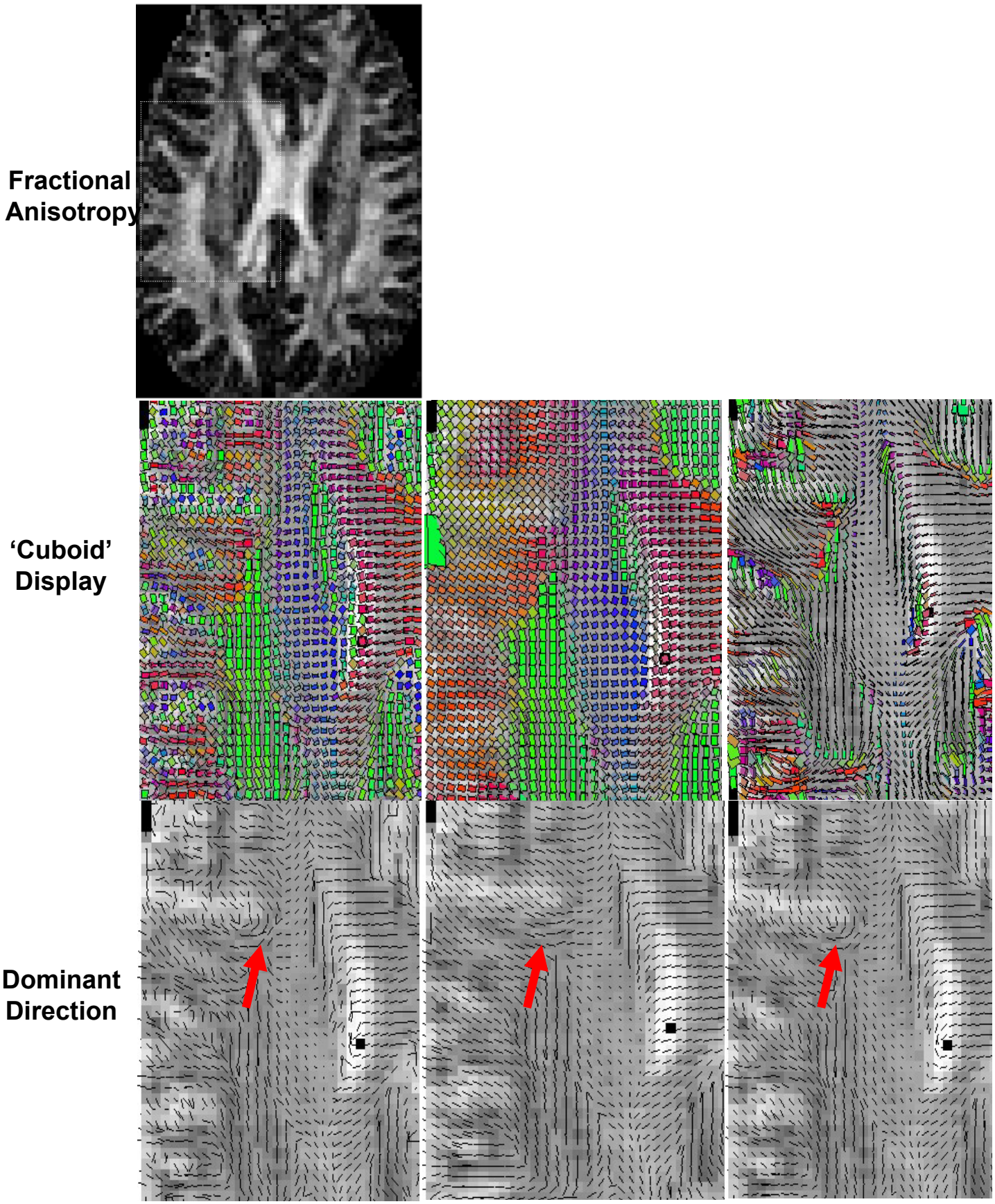
Fractional Anisotropy
'Cuboid' Display
Dominant Direction
Unsmoothed
Smoothed Normalized Tensor
Smoothed Directional Projection

Figure 4

Figure 4: Close up displays demonstrate the effect of normalized tensor (2nd column) and directional projection (3rd column) smoothing more clearly by displaying the 'cuboid' (2nd row) and dominant direction vector (3rd row) of the principle eigenvector for these two models for a portion of the cerebral hemisphere marked on fractional anisotropy display. Region above thick arrows are one example where directional projection preserves details more visibly.

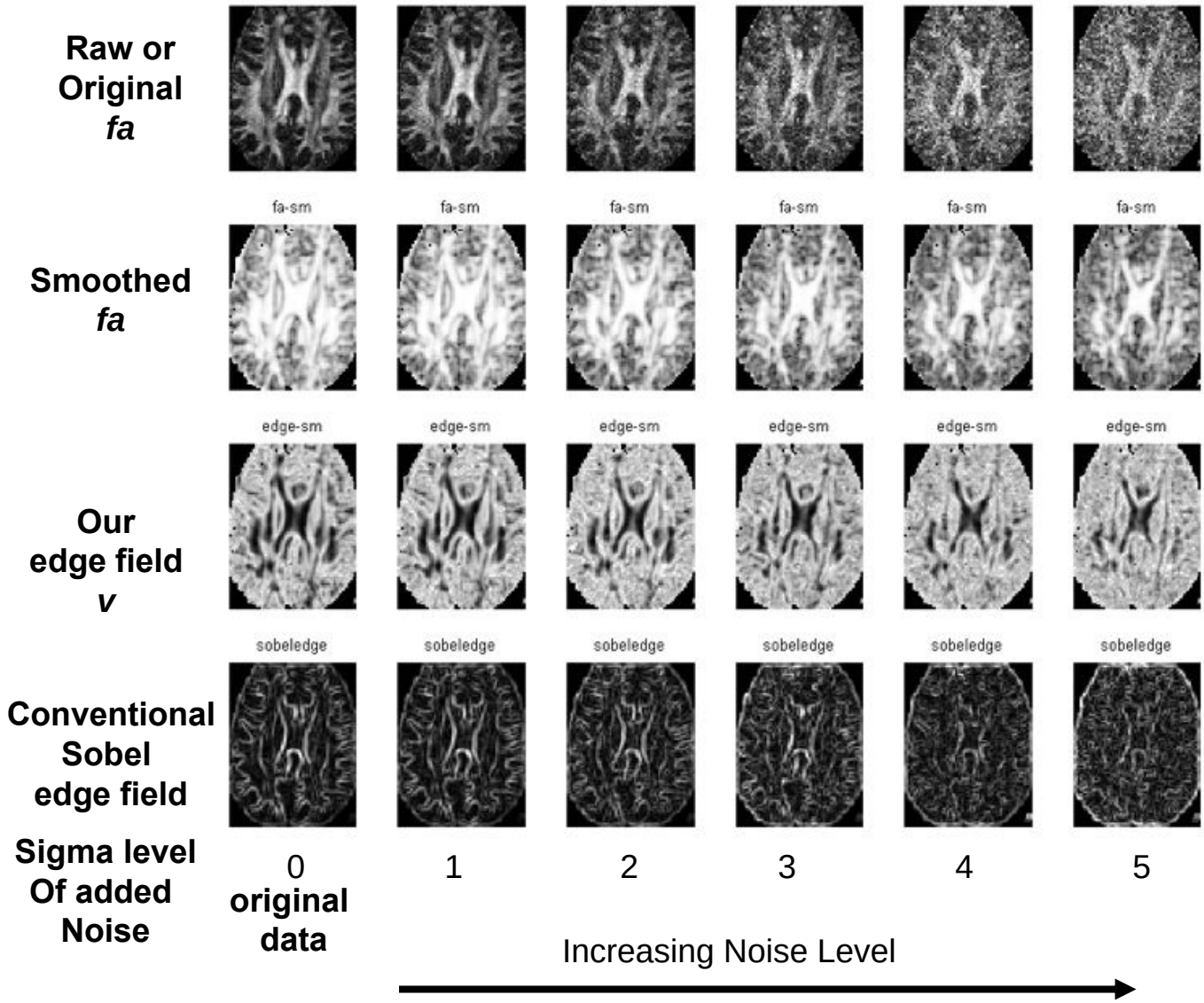

Figure 5. Effect of added noise on raw fa, smoothed fa, our edge field v, and conventional Sobel edge field. The directional projection based smoothing and segmentation (2nd and 3rd) row are more robust to added noise.

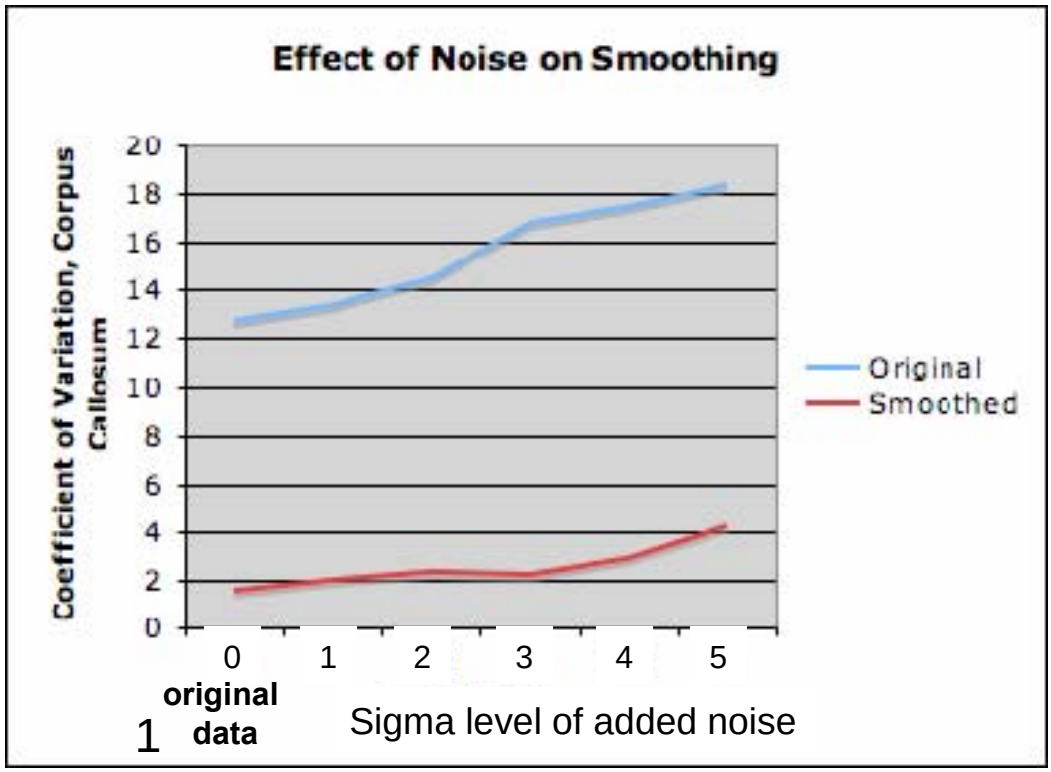

Figure 6. Effect of noise on smoothing. The coefficient of variation of the smoothed fa (bottom curve) corresponding to the second row of images in Figure 5 is significantly lower than that of the raw or original fa (top curve) corresponding to the first row of Figure 5. Curves are for corpus collosum region. Similar results obtain for other regions in Figure 3.